A Bottom-Up Approach to Red-emitting Molecular-Based Nanoparticles with Naturally Stealth Properties and their Use for Single Particle Tracking Deep in Brain Tissue

Morgane Rosendale, Jessica Flores, Chiara Paviolo, Paolo Pagano, Jonathan Daniel, Joana Ferreira, Jean-Baptiste Verlhac, Laurent Groc, Laurent Cognet*, and Mireille Blanchard-Desce**

Dr. M. Rosendale, J. Flores, Dr. P. Pagano, Dr. J. Daniel, Prof. J-B. Verlhac, Dr. M. Blanchard-Desce
Univ. Bordeaux Institut des Sciences Moléculaires (CNRS UMR 5255), 351 Cours de la Libération, 33405 Talence, France
Dr. C. Paviolo, Dr. L. Cognet
LP2N, Univ. Bordeaux, Institut d'Optique & CNRS, UMR 5298, 351 Cours de la Libération, 33405 Talence, France
Dr. J. Ferreira, Dr. L. Groc
Interdisciplinary Institute for Neuroscience, Univ. Bordeaux & CNRS, UMR 5297, 146 Rue-Léo Saignat, 33076 Bordeaux, France
E-mail: mireille.blanchard-desce@u-bordeaux.fr

Keywords: brightness, fluorescence, organic nanoparticles, single particle tracking, stealth, brain extracellular space

Fluorescent nanoparticles dedicated to bioimaging applications should possess specific properties which have to be maintained in the aqueous, reactive and crowded biological environment. These include chemical and photo-stability, small size (on the scale of subcellular structures), biocompatibility, high brightness and good solubility. The latter is a major challenge for inorganic nanoparticles, which require surface coating to be made water-soluble.[1] Molecular-based Fluorescent Organic Nanoparticles (FONs)[2] may prove a promising, spontaneously water-soluble alternative, whose bottom-up design allows for the fine-tuning of individual properties. Here, we address the critical challenge of controlling the interaction of nanoparticles with cellular membranes. We report on bright, size-tunable, red emitting, naturally stealth FONs which do not require the use of antifouling agents to impede interactions with cellular membranes. As a proof of concept, we imaged and tracked single FONs diffusing up to 150 μm deep in brain tissue.

Nanoparticles (NPs) benefit from a number of advantages over (free) fluorescent dyes including improved brightness[3] and longer vascular circulation times.[4] Inorganic NPs such as quantum-dots[5] and fluorescent polymeric NPs[6] are widely used for bioimaging applications. While QDs show remarkable brightness and photostability, they suffer from the intrinsic limitation of being water

insoluble as bare nanomaterials, thus requiring coating by hydrophilic agents.[7] Moreover, the brightest QDs include toxic components (Cd, Se, As, In …), which impedes their applicability to translational research and raises concerns for environmental clearance.[8] An interesting alternative may thus lie with molecular-based Fluorescent Organic Nanoparticles (FONs).[2,9] FONs are obtained by self-aggregation of dedicated dyes in water. Importantly, the properties of FONs can be finely tuned by molecular engineering of their constituting dyes. Red-shifted emission of FONs made from dipolar or quadrupolar dyes is usually achieved by increasing the strength of the electron donor/acceptor pair or by excitonic coupling between dye subunits. However, we have previously reported on red-shifted emission stemming from the nano-organization of dyes upon nano-aggregation.[10] We had indeed demonstrated that the emission of linear vs. branched push-pull dipolar dyes was shifted from green to red in FONs, even though their fluorescence properties in organic solvents were virtually identical, indicating that the different imposed topologies of the subunits within nano-aggregates regulate their emission properties. Remarkably, red-shifted FONs also revealed a markedly lower colloidal stability in the bloodstream than green emitting ones, resulting in acute toxicity *in vivo*.[10] These founding results unveiled the promise that operating confinement-enhanced dipolar interactions and polarization effects can tune the luminescence properties, colloidal stability and, most attractively, surface properties of FONs.[10,11] In this regard, a critical challenge specific to biomedical applications is to control the interactions between NPs and cells.[1,4,12] When subcellular compartments are to be targeted (e.g. for drug delivery), fluorescent nanoprobes should penetrate inside the cells. However, for detecting surface receptors (e.g. for diagnostics purposes) or exploring the extracellular space (ECS), they should remain outside the cells. A major field of research in which ECS exploration is currently gaining interest is neuroscience.[13] The ECS is indeed a key compartment that occupies 20-25% of the total brain volume, a fraction that varies with sleep, age and disease.[14] The challenge for the development of NPs devoted to ECS exploration is to ensure the absence of non-specific interactions with cellular membranes.[15] Surface coating or covalent grafting of PEG chains are extremely popular strategies to yield stealth inorganic

or polymeric NPs.[16] Surface modification however complicates the realization of a fully-controlled nano-bio interface. Moreover, immunogenic responses to PEG moieties are increasing as it is more and more widely used in cosmetics and drugs.[17] In this work, we demonstrate an unusual approach to obtaining inherently stealth nanoparticles based on the specific structure of FONs constitutive dyes. Thanks to the unique combination of properties of the obtained FONs, i.e. brightness, red-shifted emission, colloidal-, structural- and photo-stability, and above all intrinsic stealth behavior, we achieved deep tissue single FON tracking in organotypic brain slices.

The design of the dye building blocks of these FONs is based on a quadrupolar scheme (D-π-A-π-D). A benzothiadiazole (BDTA) electron-withdrawing moiety is used as a potent central acceptor element (A) together with two propeller shaped electron-releasing diphenylamine moieties as donor end-groups (D) (**Figure 1**A-B).

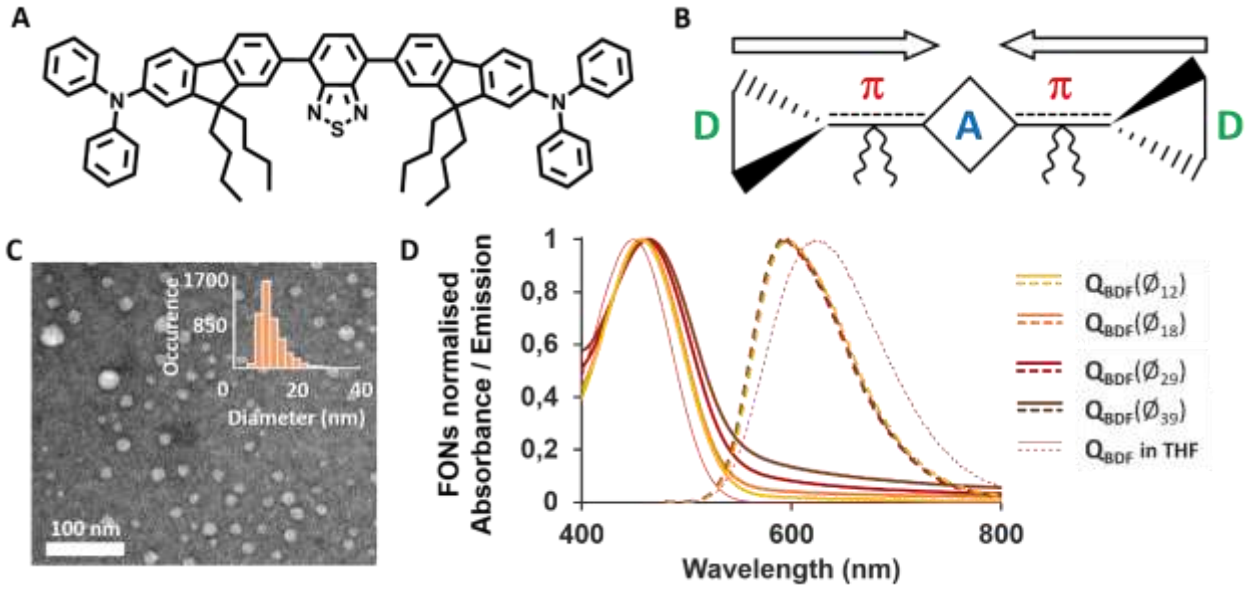

Figure 1. A Chemical structure of the **Q_{BDF}** dye. **B** Schematic of the D-π-A-π-D quadrupolar design. **C** Representative TEM image and size distribution (inset) of FONs obtained by nanoprecipitation of 0.4 mM **Q_{BDF}** dye in THF into water (1 % v/v). **D** Overlapped normalized absorbance (solid lines) and emission (dashed lines) spectra of **Q_{BDF}** dye in THF (red) and of **Q_{BDF}** FONs of different sizes (yellow to brown) prepared from varying dye stock concentrations in THF.

Such a quadrupolar scheme promotes a periphery-to-core intramolecular charge transfer (ICT) which is accountable for strong absorption. ICT is also meant to influence the self-organization of dyes upon confinement: electrostatic interactions between quadrupolar dyes are expected to promote a specific packing as compared to dipolar dyes. In addition, we chose conjugated connectors made of fluorene moieties bearing two *n*Butyl side chains. This dye is thus hereafter named **Q_{BDF}**, for Quadrupolar BDTA-Diphenylamine-Fluorene dye. The four alkyl chains extending above and below the plane of the fluorene units impose spacing between the dyes and are expected to hamper □□□ interactions between fluorene moieties as well as hinder excitonic coupling[18]. They additionally convey a marked hydrophobic character, particularly at the edges of the molecule. **Q_{BDF}** is indeed well soluble in low to medium polarity organic solvents, shows very poor solubility in polar solvents and is not soluble in water.

FONs made from **Q_{BDF}** are easily obtained by rapid addition of a minute amount of a stock solution of **Q_{BDF}** in tetrahydrofuran (THF) into a large volume of water (see supplementary information). Nanoprecipitation proceeds readily with the quasi-instantaneous formation of a transparent and colored aqueous colloidal solution. The formation of nanoparticles of spherical shape can be attested by transmission electron microscopy (TEM) (**Figure 1C, Figure S1**A, **Table S1**).

To examine the influence of NP size on their ability to diffuse into biological tissues, we modulated the FONs' size by varying the concentration of **Q_{BDF}** dye in THF prior to nano-precipitation. Stock concentrations ranging from 0.4 to 4 mM yield FONs of increasing sizes (**Table 1**). Of note, the smaller FONs, nano-precipitated from the lowest stock concentrations, show unimodal distributions with dry diameters averaging at 12 and 18 nm. In contrast, FONs originating from the more concentrated stock solutions show a bimodal distribution, yielding a mixture of two populations: very small FONs similar to the ones described above (~15 nm), and bigger FONs of broader size dispersion (~60 nm). Interestingly, all **Q_{BDF}** FONs show very negative surface potentials in water (Table 1).

Table 1. Characteristics of **Q_{BDF}** FONs of increasing size and comparison with red QDs

NPs	$Ø_{TEM}$ [a] [nm]	$Ø_{SPT}$ [b] mQ [nm]	$Ø_{SPT}$ [c] PBS + FBS [nm]	ζ [d] [mV]	N [e]
Q_{BDF} (0.4 mM)*	12	57	72	-67	532
Q_{BDF} (1 mM)*	18	72	89	-64	1796
Q_{BDF} (2 mM)*	29	84	97	-64	7510
Q_{BDF} (4 mM)*	39	100	112	-63	18266
QD605	10 x 3 **	-	-	-	-
QD655	12 x 5 **	22	-	-	-

* Stock concentration of **Q_{BDF}** dye used for nanoprecipitation is in parenthesis. a) Mean dry diameter determined by TEM. b-c) Hydrodynamic diameter determined (b) by SPT in water or (c) by SPT in PBS + 10% FBS; d) Zeta potential; e) Average number of dye molecules per FON calculated from ØTEM. ** Size measurements performed on images in [27]. Red QDs are not purely spherical: approximate sizes are indicated as length x width.

Q_{BDF} FONs were found to be strong absorbers in the blue-green visible spectral region (Figure 1D, **Table 2**). The absorption spectra of dye subunits within FONs compares well with that of molecular **Q_{BDF}** in THF (**Figure S2**, **Table S2**). Furthermore, no splitting or shoulder is observed, indicating a lack of excitonic coupling. The molar attenuation coefficient of **Q_{BDF}** FONs increases markedly with their size as is the case for QDs. Yet, their absorption spectra remain unchanged, indicating that their absorption originates from the absorption of individual dyes confined within the NPs and ruling out electron delocalization between subunits.

All **Q_{BDF}** FONs show bright fluorescence, illustrating the successful limitation of aggregation induced quenching within FONs. In contrast to QDs, their emission spectra remain virtually unchanged with increasing size (Figure 1D). Their fluorescence quantum yields, amounting to about 30 %, are relatively high for bare, red-emitting NPs in water having no protective shell. We note that **Q_{BDF}** FONs show two distinct lifetimes in the ns range. The longer one is reminiscent of that of molecular **Q_{BDF}** in THF (5.5 ns, Table S2) while the shorter might tentatively be ascribed to dyes located on the surface of the NPs as its contribution increases with decreasing size. These dyes may indeed undergo non-radiative (especially vibrational) decay processes favored by water molecules H-bonded to the surface.

Table 2. Photophysical properties of **Q_{BDF}** FONs of increasing size and comparison with red QDs

NPs	λ_{abs}^{max} a) [nm]	ε^{max} b) [10^7 M^{-1} cm^{-1}]	λ_{em}^{max} c) [nm]	Φ_f d) [%]	τ_f e) [%]	$\varepsilon^{max}.\Phi_f$ f) [10^6 M^{-1} cm^{-1}]
$Q_{BDF}(Ø_{12})$ *	458	1.4	598	29	4.6 (0.60) 1.9 (0.40)	4.0
$Q_{BDF}(Ø_{18})$	458	5.0	594	30	5.0 (0.62) 2.1 (0.38)	15
$Q_{BDF}(Ø_{29})$	462	21.2	595	33	5.5 (0.68) 2.6 (0.32)	70
$Q_{BDF}(Ø_{39})$	463	55.9	593	34	5.5 (0.69) 2.5 (0.31)	190
QD605 **	-	0.4	609	70	-	3.4
QD655 **	-	0.6	654	67	-	4.0

* Dry TEM diameter is in parenthesis; a) Absorbance maximum wavelength; b) Molar attenuation coefficient of the FONs at the absorbance maximum λ_{abs}^{max} considering N dye moieties per nanoparticle (Table 1); c) Emission maximum wavelength; d) Fluorescence quantum yield; e) Fluorescence lifetime. The contribution of each lifetime value to the fit is indicated between brackets; f) Brightness; ** QDs absorb in the UV-vis with a sharp decrease after ~ 500 nm. Here, ε^{max} was measured at λ_{abs}^{max} of **Q_{BDF}**(Ø12) for comparison.

Thanks to their intense absorption and sizeable fluorescence quantum yield, **Q_{BDF}** FONs show high brightness values, which increase significantly with size, in relation with the larger number of dyes confined within a single NP (Table 1, **Figure S3**). Importantly, the brightness of the smallest FONs (**Q_{BDF}**(Ø12)) rivals that of red emitting QDs. Moreover, **Q_{BDF}** FONs show good colloidal stability. Colloidal suspensions may indeed vary in time such that NPs fuse or aggregate as the solution matures. Yet we observe that their absorption spectra remain virtually unchanged and show no increased scattering or broadening over a month (**Figure S4**), and even up to 6 months (**Figure S5**). This indicates that FONs neither aggregate nor agglomerate. Yet complementary measurements indicate that their size distributions slowly evolve over time (**Figure S1B** and **Figure S6**) showing broadened size distribution. Interestingly, the bigger FONs (**Q_{BDF}**(Ø39), **Q_{BDF}**(Ø29)) also maintain their fluorescence quantum yield over a month, while the smaller **Q_{BDF}**(Ø18) and **Q_{BDF}**(Ø12) respectively maintain 70% and 50% of their fluorescence over a month (Figure S5). This suggests that slow surface rearrangements and exchange of the dyes from the surfaces of the NPs occur over time.

Based on the remarkable brightness of these FONs in aqueous medium, we evaluated their usability for single particle tracking (SPT). We first assessed that they were photo-stable enough to remain detectable for around a minute under illumination (**Figure 2**A), an adequate time window to extract diffusion parameters.[19] We then detected FONs as freely moving puncta in water (**Movies S1** to **S4**) whose Brownian motion could be tracked in post-acquisition image analysis (Figure 2B, **Movie S5**), allowing us to determine the hydrodynamic diameter of FONs (Table 1, **Table S3**, **Figure S7**A). In doing so, we made a thought-provoking observation: the hydrated diameters of $\mathbf{Q_{BDF}}$ FONs in water are substantially larger than their dry ones. This suggests the formation of a network of organized water molecules at the surface of FONs forming a polar, self-coating shell. Such behavior is reminiscent of the structuration of water molecules coating phospholipid bilayers.[20] Interestingly, we had previously reported a similar 50 nm increase in the hydrated diameter of FONs made from a different quadrupolar dye.[21] In contrast, we had reported that FONs composed of related dipolar[22] or bis-dipolar[23] dyes, bearing the same electron-donor moieties, displayed comparable dry and hydrated diameters. We next tracked FONs in Phosphated Buffered Saline (PBS, pH 7.4) supplemented with 10% Foetal Bovine Serum (FBS) (Table 1, **Table S4**, Figure S7B) to investigate the possible formation of a protein corona. Interestingly, the presence of serum proteins generates a comparatively small increase in size, suggesting that the "ice" shell may buffer the direct interaction of the FONs' surface with proteins. Finally, we assessed the versatility of FONs under various pH and osmolarity conditions by confirming their integrity in two other physiologically relevant buffers: MES Buffered Saline (MBS, pH 5.5, 310 mosm) used to mimick the acidic intravesicular environment and Artificial CerebroSpinal Fluid (ACSF, pH 7.4, 280 mOsm) routinely used for neuronal cultures, both supplemented with 10% FBS. We found that under either condition, FONs could be detected as punctate emitters of similar hydrodynamic diameter as in PBS + FBS (**Table S5, Figure S8**).

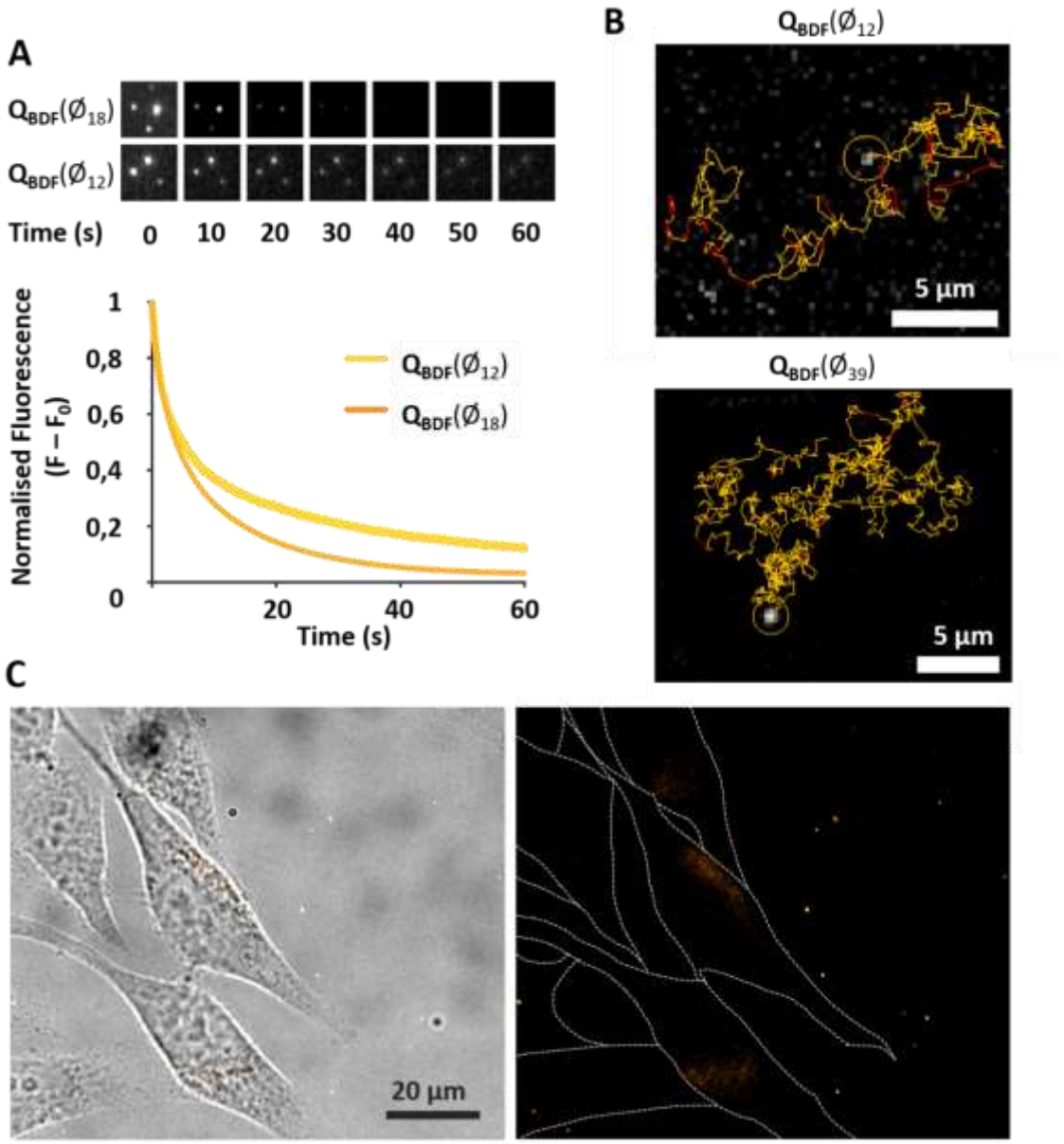

Figure 2. A (Top) Example regions of interest and (Bottom) average trace of $\mathbf{Q_{BDF}}$ FONs intensity decaying with time. **B** Example trajectory of a single $\mathbf{Q_{BDF}}$(Ø12) (Top) and $\mathbf{Q_{BDF}}$(Ø39) (Bottom) FON in water. **C** Example fluorescence image of $\mathbf{Q_{BDF}}$(Ø18) FONs incubated for 24h with HeLa cells; (Left) overlaid with a bright field image. (Right) with cell contours traced for clarity.

Following on these results, we assessed the biocompatibility and observed the behavior of $\mathbf{Q_{BDF}}$ FONs in a cellular environment. We found that after 24 h incubation with HeLa cells in serum-containing culture medium, they did not stick to cell surfaces, indicating a lack of interaction with biological membranes (Figure 2C, **Figure S9**). They also did not accumulate intracellularly, demonstrating that the specific $\mathbf{Q_{BDF}}$ dye design generates inherently stealth FONs that are not taken up by endocytosis. This behavior is rather unique in that the majority of FONs reported in the literature tend to be

internalized by cells, including FONs made from dipolar[22,24] or quadrupolar[21,25] dyes having similar donor and/or acceptor groups. It is however reminiscent of recent reports on FONs made from bis-dipolar[23] or quadrupolar[26] dyes bearing fluorene-linked aliphatic pendant chains. Of note, most of those FONs also showed negative surface potentials, indicating that the stealth behavior of **Q$_{BDF}$** FONs does not originate from the surface potential alone. This finding emphasizes the fact that the surface of a nanoparticle is crucial to its stealth behavior. As the specific bottom-up design of the dye tunes the nature of the interface between the FONs surface and the surrounding water molecules, the combination of the quadrupolar electronic charge distribution along the long axis and the presence, close to the edges of the dye, of long hydrophobic alkyl chains appears to be a determining factor. This finding unveils an original bottom-up route for engineering intrinsic stealth properties of FONs. Considering the unique set of properties of bare **Q$_{BDF}$** FONs, we next investigated whether they could be used to explore the extracellular space of living tissues. We used hippocampal organotypic brain slices (**Figure 3**A) as a model system in which neuronal connectivity is partially maintained but where deep tissue imaging remains challenging. Recording depth is indeed critical in this system, as superficial layers of tissue may have reorganized after the slicing procedure. We focused our attention on the smaller FONs and observed that NPs of different sizes behave differently. After 2h incubation, **Q$_{BDF}$**(Ø18) FONs could not satisfyingly penetrate inside the tissue. Most FONs were found near the surface of the slices and the few that were detectable at depth appeared immobile. In sharp contrast, **Q$_{BDF}$**(Ø12) FONs were able to penetrate brain slices without excessively accumulating at the surface of the tissue, in a similar fashion to QD-655(Ø12x5) which we used for comparison (**Movies S6-S7**). Moving QDs could reliably be imaged at various depths up to 80 μm. Under the same conditions, we recorded several freely moving **Q$_{BDF}$**(Ø12) FONs up to 60 μm in depth as well as a few events past 80 μm and up to 150 μm deep (Figure 3B-C, **Figure S10**). Hence, **Q$_{BDF}$** nanoparticles represent a new state-of-the-art nanotool for bioimaging deep in tissues, offering a non-toxic, ecofriendly alternative to heavy metal containing QDs.

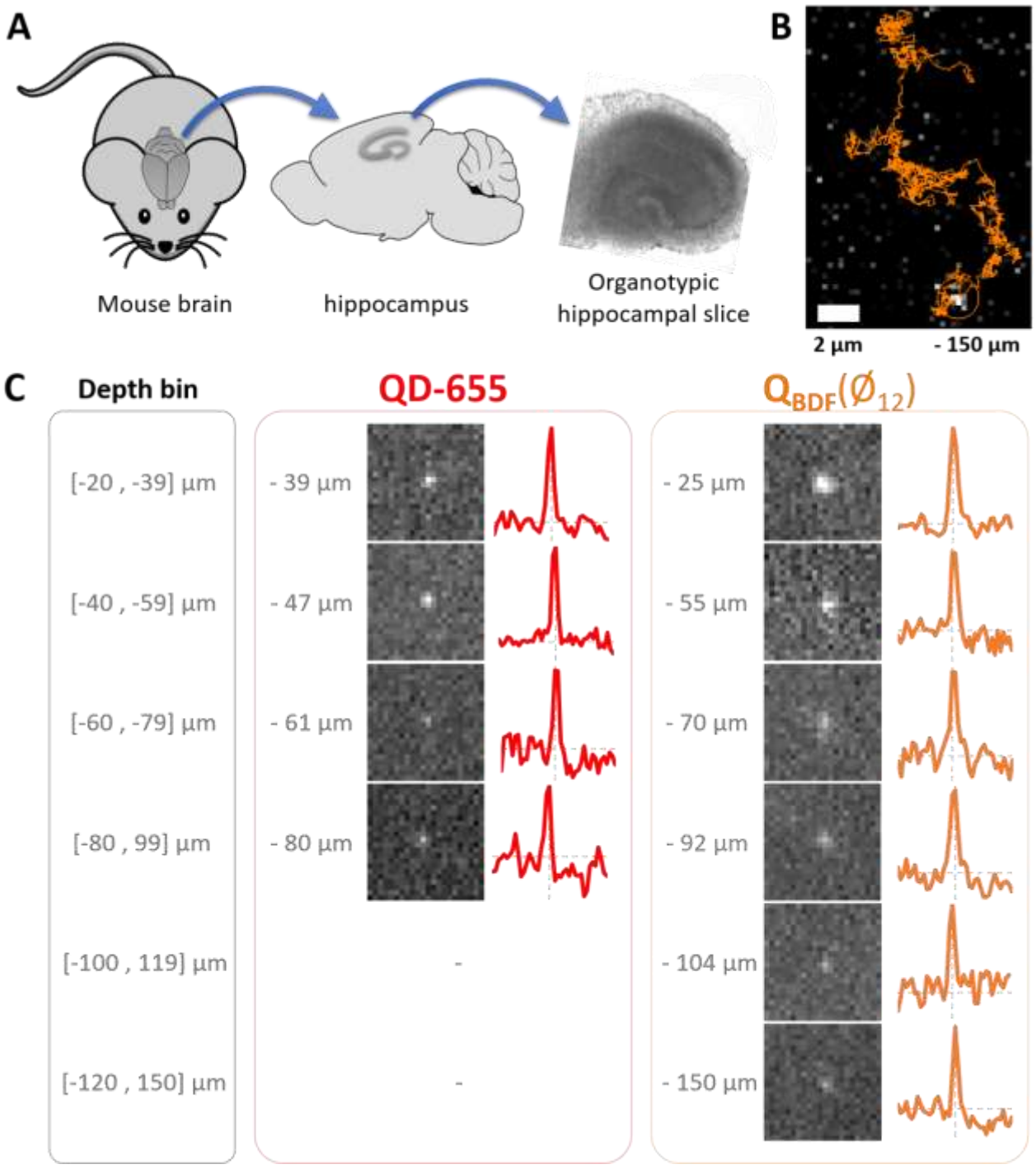

Figure 3. A Schematic of organotypic brain slices preparation after extraction of the mouse brain and dissection of the hippocampus. **B** Example trace of a $\mathbf{Q_{BDF}}$(Ø12) FON recorded for 11 s, 150 µm below the surface of a brain slice. **C** Example fluorescence images of QDs and FONs recorded at the indicated depths. To the right of each image, an intensity profile going from left to right of the brightest pixel is provided.

We have therefore shown that stealth, bright, water-soluble, red-emitting, all organic nanoemitters of small size can be obtained by self-aggregation of specific quadrupolar dyes exhibiting strong ICT and

decorated with four lipophilic pendant chains. Remarkably, the spontaneously stealth behavior of **Q_{BDF}** FONs is singular and contrasts with previous reports on FONS, including FONs made from dipolar and quadrupolar dyes that are used for intracellular imaging. Importantly, **Q_{BDF}** FONs require no PEG coating to achieve stealth behavior which simplifies the preparation of nanoprobes, reduces their complexity and allows greater control of their final size. Indeed, **Q_{BDF}** FONs can be made extremely small, down to ~ 10 nm, i.e. roughly the size of an antibody, allowing for deep tissue imaging. Expanding our understanding of these FONs behavior in biological environments will be of the highest interest from a theoretical point of view, as the specific nature of the dye is obviously playing a major role. In particular, the intimate nature of the nanoparticle surface and subnano-rugosity effects may be involved in the structuration of the nano-interface. Also, the technical feat of observing single spherical (0-D) nanoparticles more than 100 μm deep in tissue has seldom been reported. Further studies will be needed to systematically investigate whether at such depths, the ECS of the brain is influenced by various parameters such as local osmolarity, network excitability or animal experience prior to brain slicing. Furthermore, the molecular design of FONs allows for finely tuned structural modifications such that several approaches can be envisaged for surface modification or biofunctionalization of these nanoparticles. These exciting possibilities w lead the way for safe, all organic bioimaging.

Supporting Information
Supporting Information is available from the Wiley Online Library or from the author.

Acknowledgements
This work received funding from the European Union's Horizon 2020 research and innovation program under the Marie Skłodowska-Curie grant agreement Nos. 841379 and 793296 to M.R. and C.P. J.Fl. was supported by the US-France-Belgium iREU Site in Translational Chemistry (NSF Grant No. 1560390). M.B-D. acknowledges support from Conseil Régional d'Aquitaine (Chaire d'accueil). We thank Agence Nationale de la Recherche (ANR-15-CE16-0004) and IdEx Bordeaux (ANR-10-IDEX-03-02). Transmission electron microscopy was done in the Bordeaux Imaging Center, a service unit of the CNRS-INSERM and Bordeaux University, member of the national infrastructure France Bioimaging (ANR-10-INBS-04).

Received: ((will be filled in by the editorial staff))
Revised: ((will be filled in by the editorial staff))
Published online: ((will be filled in by the editorial staff))

References

[1] L. Guerrini, R. A. Alvarez-Puebla, N. Pazos-Perez, *Materials* **2018**, *11*, 1154.
[2] D. Svechkarev, A. M. Mohs, *Curr. Med. Chem.* **2019**, *26*, 4042.
[3] U. Resch-Genger, M. Grabolle, S. Cavaliere-Jaricot, R. Nitschke, T. Nann, *Nat. Methods* **2008**, *5*, 763.
[4] L. A. Lane, X. Qian, A. M. Smith, S. Nie, *Annu Rev Phys Chem* **2015**, *66*, 521.
[5] A. M. Wagner, J. M. Knipe, G. Orive, N. A. Peppas, *Acta Biomaterialia* **2019**, *94*, 44.
[6] Y. Braeken, S. Cheruku, A. Ethirajan, W. Maes, *Materials* **2017**, *10*, 1420.
[7] O. S. Wolfbeis, *Chem. Soc. Rev.* **2015**, *44*, 4743.
[8] T. L. Rocha, N. C. Mestre, S. M. T. Sabóia-Morais, M. J. Bebianno, *Environ. Int.* **2017**, *98*, 1.
[9] a) D. Horn, J. Rieger, *Angew. Chem. Int. Ed. Engl.* **2001**, *40*, 4330; b) S. Fery-Forgues, *Nanoscale* **2013**, *5*, 8428; c) W. A. Wani, M. Shahid, A. Hussain, M. F. AlAjmi, *Fluorescent Organic Nanoparticles: New Generation Materials with Diverse Analytical and Biomedical Applications*, Springer Singapore **2018**; d) E. Ishow, A. Brosseau, G. Clavier, K. Nakatani, P. Tauc, C. Fiorini-Debuisschert, S. Neveu, O. Sandre, A. Léaustic, *Chem. Mater.* **2008**, *20*, 6597.
[10] V. Parthasarathy, S. Fery-Forgues, E. Campioli, G. Recher, F. Terenziani, M. Blanchard-Desce, *Small* **2011**, *7*, 3219.
[11] a) C. Mastrodonato, P. Pagano, J. Daniel, M. Vaultier, M. Blanchard-Desce, *Molecules* **2016**, *21*, 1227; b) K. Amro, J. Daniel, G. Clermont, T. Bsaibess, M. Pucheault, E. Genin, M. Vaultier, M. Blanchard-Desce, *Tetrahedron* **2014**, *70*, 1903.
[12] R. L. Pinals, L. Chio, F. Ledesma, M. P. Landry, *Analyst* **2020**, *145*, 59090.
[13] a) R. G. Thorne, C. Nicholson, *Proc. Natl. Acad. Sci. U.S.A.* **2006**, *103*, 5567; b) S. Hrabetova, L. Cognet, D. A. Rusakov, U. V. Nägerl, *J. Neurosci.* **2018**, *38*, 9355.
[14] E. Syková, *Neuroscience* **2004**, *129*, 861.
[15] J. W. Shreffler, J. E. Pullan, K. M. Dailey, S. Mallik, A. E. Brooks, *International Journal of Molecular Sciences* **2019**, *20*, 6056.
[16] J. S. Suk, Q. Xu, N. Kim, J. Hanes, L. M. Ensign, *Advanced Drug Delivery Reviews* **2016**, *99*, 28.
[17] J. J. F. Verhoef, T. J. Anchordoquy, *Drug Deliv. and Transl. Res.* **2013**, *3*, 499.
[18] N. J. Hestand, F. C. Spano, *Chem. Rev.* **2018**, *118*, 7069.
[19] L. Groc, M. Lafourcade, M. Heine, M. Renner, V. Racine, J.-B. Sibarita, B. Lounis, D. Choquet, L. Cognet, *J. Neurosci.* **2007**, *27*, 12433.
[20] M. Prats, J.-F. Tocanne, J. Teissié, *Biochimie* **1989**, *71*, 33.
[21] J. Daniel, A. G. Godin, M. Palayret, B. Lounis, L. Cognet, Mireille Blanchard-Desce, *J. Phys. D: Appl. Phys.* **2016**, *49*, 084002.
[22] E. Genin, Z. Gao, J. A. Varela, J. Daniel, T. Bsaibess, I. Gosse, L. Groc, L. Cognet, M. Blanchard-Desce, *Adv. Mater.* **2014**, *26*, 2258.
[23] M. Rosendale, G. Clermont, J. Daniel, C. Paviolo, L. Cognet, J.-B. Verlhac, M. Blanchard-Desce, in *Neurophotonics*, International Society For Optics And Photonics, **2020**, p. 1136005.
[24] a) A. Faucon, H. Benhelli-Mokrani, L. A. Córdova, B. Brulin, D. Heymann, P. Hulin, S. Nedellec, E. Ishow, *Advanced Healthcare Materials* **2015**, *4*, 2727; b) D. Wang, H. Su, R. T. K. Kwok, X. Hu, H. Zou, Q. Luo, M. M. S. Lee, W. Xu, J. W. Y. Lam, B. Z. Tang, *Chem. Sci.* **2018**, *9*, 3685; c) J. Boucard, T. Briolay, T. Blondy, M. Boujtita, S. Nedellec, P. Hulin, M. Grégoire, C. Blanquart, E. Ishow, *ACS Appl. Mater. Interfaces* **2019**, *11*, 32808.
[25] J. Zhang, R. Chen, Z. Zhu, C. Adachi, X. Zhang, C.-S. Lee, *ACS Appl. Mater. Interfaces* **2015**, *7*, 26266.
[26] A. H. A. M. van Onzen, L. Albertazzi, A. P. H. J. Schenning, L.-G. Milroy, L. Brunsveld, *Chem. Commun.* **2017**, *53*, 1626.
[27] B. N. G. Giepmans, S. R. Adams, M. H. Ellisman, R. Y. Tsien, *Science* **2006**, *312*, 217.

TOC

Fluorescent organic nanoparticles displaying intrinsic stealth properties towards biological membranes are prepared by nanoprecipitation of a hydrophobic, conjugated, red-emitting quadrupolar dye. The excellent brightness, stability and size control down to ~10 nm of these nanoparticles allow for single particle tracking deep in brain tissue. These findings point to a novel route for the bottom-up molecular design of the nano-bio interface.

Keyword
Brightness, brain extracellular space, nanoparticles, single particle tracking, stealth

A Bottom-Up Approach to Red-emitting Molecular-Based Nanoparticles with Naturally Stealth Properties and their Use for Single Particle Tracking Deep in Brain Tissue

Morgane Rosendale, Jessica Flores, Chiara Paviolo, Paolo Pagano, Jonathan Daniel, Joana Ferreira, Jean-Baptiste Verlhac, Laurent Groc*, Laurent Cognet*, and Mireille Blanchard-Desce*

Graphical Abstract

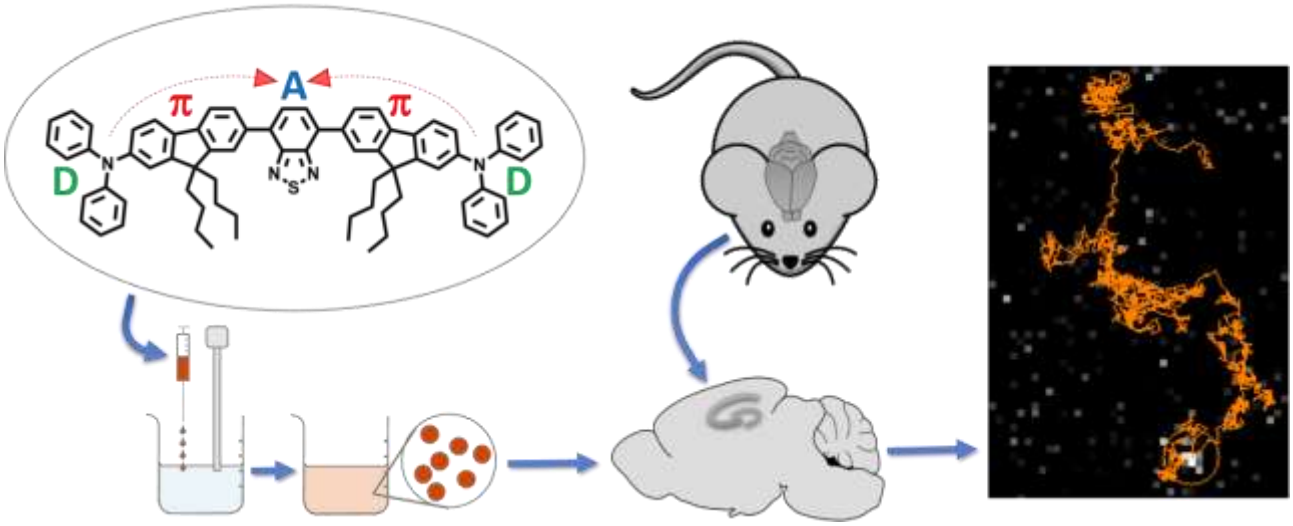

Caption: Naturally made stealth ultra-bright organic nanoparticles allow for Single Particle Tracking Deep in Brain Tissue